

Continuous variable qumodes as non-destructive probes of quantum systems

Thomas J. Elliott,^{1, 2,*} Mile Gu,^{1, 3, 4} Jayne Thompson,⁴ and Nana Liu^{2, 4, 5, †}

¹*School of Physical and Mathematical Sciences, Nanyang Technological University, Singapore 639673*

²*Department of Physics, Clarendon Laboratory, University of Oxford,
Parks Road, Oxford OX1 3PU, United Kingdom*

³*Complexity Institute, Nanyang Technological University, Singapore 639673*

⁴*Centre for Quantum Technologies, National University of Singapore, 3 Science Drive 2, Singapore 117543*

⁵*Singapore University of Technology and Design, 8 Somapah Road, Singapore 487372*

(Dated: December 14, 2024)

With the rise of quantum technologies, it is necessary to have practical and preferably non-destructive methods to measure and read-out from such devices. A current line of research towards this has focussed on the use of ancilla systems which couple to the system under investigation, and through their interaction, enable properties of the primary system to be imprinted onto and inferred from the ancillae. We propose the use of continuous variable qumodes as ancillary probes, and show that the interaction Hamiltonian can be fully characterised and directly sampled from measurements of the qumode alone. We suggest how such probes may also be used to determine thermodynamical properties, including reconstruction of the partition function. We show that the method is robust to realistic experimental imperfections such as finite-sized measurement bins and squeezing, and discuss how such probes are already feasible with current experimental setups.

The impressive developments in methods for exerting control over quantum systems in recent years have made the realisation of technologies that exploit truly quantum phenomena a very imminent reality. The candidate systems that may be used for this paradigm are numerous, among which include are ultracold atoms [1], ion traps [2], superconducting circuits [3], and microwave cavities [4]. These technologies can then be put to task enhancing computation, simulation, and metrology [5–9].

A necessary aspect of a quantum technology is to read-out the result output by the system. However, in many of the proposed architectures this process is destructive to the system, allowing only a single-shot reading, after which the system must be completely re-prepared. For example, with cold atom systems, a widely-used measurement method is time-of-flight [10–13], which involves destruction of the atomic trapping potential, hence requiring the atoms to then be re-trapped and re-cooled. Moreover, in other systems direct methods to measure particular sets of observables may not be available.

A recent proposal towards circumventing this involves coupling the system to ancillae. Through their interaction, properties of the system are imprinted onto the ancillae [14, 15], and information about the system may then be obtained through measurement of the ancillae alone [16–28]. While such measurements disturb the system state and are hence not non-demolition, they do not destroy the system. This method has been explored in particular for cold atom systems, where atomic impurities form ancilla qubits [29]; post-processing of the impurity measurement statistics then allows properties such as density [26] and temperature [21, 27] to be determined.

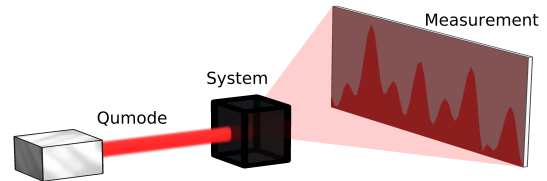


FIG. 1: **Probing quantum systems with qumodes.** A continuous variable qumode illuminates a system of interest, inheriting properties of the system through their interaction. The state of the qumode is then measured, revealing information about the system.

In parallel, developments in continuous variable quantum information processing [30–34], based on ‘qumodes’ rather than qubits, provide new applications for quantum optics and collective atomic phenomena in quantum technologies. One recently proposed model of quantum computation uses squeezed qumodes as a resource for phase estimation of an operator [35].

We unite these two themes, and investigate the use of continuous variable qumode ancillae to probe quantum systems [Fig. 1]. We find that for an appropriate initial qumode state, the statistics of the system operator by which the qumode couples to the system are mapped directly onto the qumode state. Subsequent measurement of the qumode then allows for the spectrum of the system operator to be determined, along with the populations of the respective eigenstates. This enables a full characterisation of the moments of the operator, as though one had directly sampled the observable from the system.

We first describe the protocol, and demonstrate how the operator statistics are imprinted onto the qumode state. We then show that the protocol is robust to ex-

*Electronic address: physics@tjelliott.net

†Electronic address: nana.liu@quantumlah.org

perimental limitations of finite squeezing of the initial qumode state and measurement bin-size. We discuss how the probes may be applied to measure thermodynamical quantities in both equilibrium and far from equilibrium settings. These include the system temperature, the partition function, free energy, heat capacity, work distributions as well as some signatures for quantum phase transitions. Finally, we propose candidate systems and system operators for which the protocol may be realisable with current experiments.

Qumode Probes. The use of qumode probes allows for the determination of the eigenvalues of an observable of a system of interest. It further allows one to measure the occupation probabilities of the associated eigenstates for the particular system state. This may be achieved even when there is no *a priori* knowledge of the system state, or the eigenvalues or eigenstates of the system operator. From the measurement of these eigenvalues and occupation probabilities, we can estimate the moments of the observable, allowing for its characterisation with respect to the (possibly unknown) system state.

The qumode probing protocol consists of three components. The first of these is the system under investigation, which is described by some generic state ρ_{sys} . The protocol does not in general need a particular form for the system or its state, and it may inhabit a discrete or continuous Hilbert space. The second component is the continuous variable qumode, described by its quadratures x and p , often referred to as ‘position’ and ‘momentum’ [36]. We shall take these quadratures to be in their dimensionless form (that is, in terms of the creation and annihilation operators a and a^\dagger of the mode, we have $x = (a + a^\dagger)/2$ and $p = (a - a^\dagger)/2i$).

The final component is the interaction between system and qumode. We shall consider an interaction Hamiltonian of the form $gx \otimes H_{\text{int}}$, where the first subspace belongs to the qumode, and the second the system [35]. Hence, the interaction acts on the system, with a strength that depends on the qumode position quadrature, with g an overall coupling strength. The associated evolution operator (in natural units $\hbar = 1$) is $U(t) = \exp(-igx \otimes H_{\text{int}}t)$, and thus the qumode is dephased in this quadrature, at a rate dependent on the the system operator H_{int} , thence motivating the use of a phase estimation-type algorithm.

We label the eigenstates of the system operator H_{int} as $|u_n\rangle$, with associated eigenvalues E_n . Thus, when the system is in such an eigenstate, and the qumode in a quadrature eigenstate $|x\rangle$, the effect of the interaction can be written

$$|x\rangle \otimes |u_n\rangle \rightarrow e^{-igxE_nt}|x\rangle \otimes |u_n\rangle. \quad (1)$$

In general, the qumode can be in a superposition of the quadrature eigenstates $|\psi_q\rangle = \int dx G(x)|x\rangle$, and the system state can always be expressed in the basis defined by the eigenstates of H_{int} : $\rho_{\text{sys}} = \sum_{mn} c_{mn} |u_m\rangle \langle u_n|$. Owing to the linearity of quantum mechanics, Eq. (1) can be extended to such states, and one can perform a

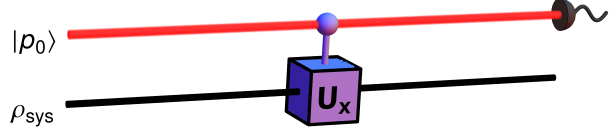


FIG. 2: **Quantum circuit for qumode probing.** A qumode prepared in momentum eigenstate $|p_0\rangle$ interacts with the system through a controlled gate $U_x = \exp(-igxH_{\text{int}}t)$ dependent on the qumode position quadrature x . Measuring the qumode in the momentum quadrature then directly samples the statistics of the system operator H_{int} for state ρ_{sys} .

partial trace over the system to obtain an expression for the qumode state after running the interaction for a time t :

$$\rho_q(t) = \int \int dx dx' G(x) G^*(x') L(x, x', t) |x\rangle \langle x'|, \quad (2)$$

where analogous to the qubit probe protocols [26, 27], we define the dephasing function $L(x, x', t) \equiv \text{Tr}(\rho_{\text{sys}} \exp(-ig(x - x')H_{\text{int}}t)) = \sum_n P_n \exp(-ig(x - x')E_n t)$, where $P_n = c_{nn}$. This is resemblant of a characteristic function for the system operator.

Let us now consider that after an interaction time τ a measurement is made of the qumode state. Inspired by the qubit-based protocols, we shall measure in a basis conjugate to that which defines the interaction Hamiltonian, here the momentum quadrature. Further, we shall for now consider the initial qumode state to have been prepared in a momentum eigenstate $|p_0\rangle = (1/\sqrt{2\pi}) \int dx \exp(ip_0 x)|x\rangle$. This protocol is illustrated in Fig. 2. Then, the probability of the measurement resulting in the outcome $|p\rangle$ is given by (see Technical Appendix)

$$P(p) = \langle p | \rho_q(\tau) | p \rangle = \sum_n P_n (\delta(p - (p_0 - gE_n \tau)))^2. \quad (3)$$

Thus, the probability distribution $P(p)$ is non-zero only at the points $p = p_0 - gE_n \tau$, where it takes values P_n . The measurement of the qumode state hence directly samples the same distribution as that of a measurement of the operator H_{int} on the state ρ_{sys} , with the mapping from qumode measurement outcomes to the spectrum of the system operator given by $E = (p_0 - p)/g\tau$. With repeated measurements, one can then obtain an estimate of the probability distribution $P(p)$ (and hence $P(E)$). This thus allows for the estimation of the spectrum, and the moments of the system operator $\langle H_{\text{int}}^m \rangle = \sum_n P_n E_n^m$. In contrast to the analogous qubit probing protocols, here these properties can be obtained directly, without the need for post-processing of the measurement outcomes.

A caveat to the above is that we have neglected the presence of the natural evolution of the system under its bare Hamiltonian H_0 during the running of the protocol.

For this to be valid, we require that the interaction occurs on timescales much faster than the natural evolution ($gH_{\text{int}} \gg H_0$), and that the natural evolution has negligible effect on the system state during the running of the protocol ($H_0\tau \ll 1$), hence imposing a maximum allowable running time for the protocol. These restrictions are lifted when the bare Hamiltonian and the interaction Hamiltonian commute, in which case the natural evolution does not affect the outcome of the qumode measurement.

Robustness to experimental imperfections. The above derivation of the qumode state after performing the protocol assumed an initial qumode state prepared in a momentum quadrature eigenstate. In practice, one can only achieve approximations to such an initial state. Specifically, there is a finite resolution ('bin'-size) in the precision with which one can measure the momentum quadrature, and only a finite level of squeezing in a given quadrature (with a quadrature eigenstate corresponding to an infinite squeezing). We can generalise the above results to encompass each of these imperfections, and thus determine the regime of parameters for which the protocol is valid. This is done by considering different initial qumode states $G(x)$ corresponding to finite bins and squeezed states.

First, we consider the case where there is a finite bin size for the quadrature measurement. A bin size of L centered on p_0 will constrain the initial momentum quadrature value p_0+k to be within the range $-L/2 \leq k \leq L/2$, and hence we can express the initial state as

$$G(x) = \frac{1}{\sqrt{2\pi L}} \int_{-\frac{L}{2}}^{\frac{L}{2}} dk e^{i(p_0+k)x}. \quad (4)$$

With this initial distribution, the final probability distribution for the qumode measurement is given by (see Technical Appendix)

$$P(p) = \sum_n \begin{cases} \frac{P_n}{L} & -\frac{L}{2} \leq p - p_0 + gE_n\tau \leq \frac{L}{2} \\ 0 & \text{otherwise.} \end{cases} \quad (5)$$

The further consequence of a finite bin size in the final measurement of the qumode can also be accounted for, by integrating this probability over the size of each bin.

For the second case, with finite squeezing, we consider an initial distribution with a Gaussian uncertainty in the value of the momentum quadrature, centred on p_0 :

$$G(x) = \left(\frac{s^2}{\pi}\right)^{\frac{1}{4}} \frac{1}{\sqrt{2\pi}} e^{ip_0x} \int dq e^{-\frac{s^2 q^2}{2}}. \quad (6)$$

Here, s corresponds to the dimensionless squeezing factor [35], parameterising the squeezing in the momentum quadrature (note that $s = 1$ corresponds to the case of an unsqueezed coherent state, defined as the eigenstate of the annihilation operator; $a|\alpha\rangle = \alpha|\alpha\rangle$). Inserting this in to Eq. (2) and following through the protocol (see Technical Appendix), we find the final probability distribution

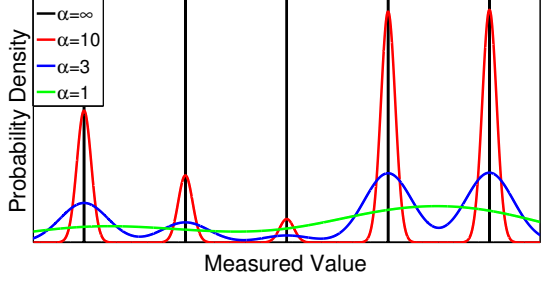


FIG. 3: **Effect of finite squeezing.** Without perfect squeezing, the distribution sampled by measuring the qumode is spread around the actual distribution of the interaction Hamiltonian. This is illustrated for various levels of precision $\alpha = \Delta/s\tau$, where Δ is the difference between the eigenvalues of H_{int} . This example H_{int} has 5 evenly-spaced eigenstates with randomly-selected populations.

for the qumode is given by

$$P(p) = \frac{s}{\sqrt{\pi}} \sum_n P_n e^{-s^2(p-p_0+g\tau E_n)^2}. \quad (7)$$

The forms of the final probability distributions Eqs. (5) and (7) are somewhat unsurprising, as they mirror the uncertainty in the initial momentum distribution; that is, the distribution of the initial momentum quadrature value p_0 ultimately defines the uncertainty in p for the final distributions. Because of these finite uncertainties in the initial momentum, the final probability distributions are no longer perfectly identical to the distribution of the system operator H_{int} , and inherit the uncertainty in the initial state. With finite measurement bin sizes, we are limited to a resolution in p of L , corresponding to a limit in the resolution of the spectrum of H_{int} of $\Delta E = L/g\tau$. For the case of finite squeezing, the squeezing factor defines the spread of the final distribution, with greater squeezing narrowing the distribution. The standard deviation of the final momentum distribution is given by $\sigma_p = \sqrt{2}/s$, corresponding to a standard deviation for the system operator eigenvalues of $\sigma_E = \sqrt{2}/s\tau$. Thus, the precision to which we can measure can be increased in both cases by running the protocol for longer or increasing the coupling strength, and by decreasing the bin size or increasing the squeezing for each of the individual cases respectively. These values for ΔE and σ_E can be replaced by our desired limit on accuracy to define the valid parameter regime. We illustrate the consequence of different levels of precision in Fig. 3.

Interestingly, we note that as with the proposal for power of one qumode computation [35], one can trade off a decreased squeezing with increased running time τ , and vice versa. While it is tempting to then conclude that these uncertainties in the final distribution can thus be negated by a sufficiently increased running time, this is not necessarily the case in general, due to the constraint imposed on τ for the effects of the system's natural evolution H_0 to be neglected.

Applications for Thermodynamics. When the system is known to be in a thermal state $\rho_\Theta(\beta) = \exp(-\beta H_\Theta)/Z(\beta)$ with respect to a Hamiltonian H_Θ , it is possible to use the qumode as a thermodynamical probe, by engineering H_{int} to be proportional to this H_Θ . Here, $\beta = 1/T$ is the inverse temperature (we employ units in which Boltzmann's constant $k_B = 1$), and $Z(\beta) = \text{Tr}(\exp(-\beta H_\Theta))$ is the partition function. In particular, note that this can be achieved even when the system is thermalised with respect to its natural Hamiltonian H_0 . In this case, because the interaction Hamiltonian will be proportional to the natural Hamiltonian, the two hence commute and there will be no restriction on the magnitude of g or the time for which the protocol can be run, as noted above.

To see this, consider that we estimate from the protocol the eigenvalues $\{E_n\}$ of H_Θ , along with their respective probabilities P_n for the state $\rho_\Theta(\beta)$. One can then construct for each eigenvalue (with degeneracy g_n) an equation of the form

$$\log(Z(\beta)) + \beta E_n = \log(g_n/P_n). \quad (8)$$

Suppose we assume known values of only two degeneracies g_{n_0}, g_{n_1} . Since Eq. (8) can be rewritten $\beta = \log(P_{n_0}g_{n_1}/(P_{n_1}g_{n_0}))/ (E_{n_1} - E_{n_0})$, we see that the qumode probe can be used as a non-destructive thermometer for quantum systems. While traditional thermometry relies on thermal equilibrium to be established between the system and the probe [37], here the temperature can be measured without this constraint. Similar probes using qubits [21, 27] instead of a qumodes also do not require equilibration. However, using a qumode as a thermometer has the advantage of being able to tune the precision through the amount of squeezing of the probe itself. Precision is thus not constrained by the number of probes themselves, which can be a limitation even for thermometers that exploit quantum advantages in precision using quantum metrology [21, 38].

When the effects of finite squeezing and bin size are considered, it is necessary that we can resolve between different eigenvalues of the interaction Hamiltonian (i.e. $\min(E_n - E_{n'}) \gtrsim \sigma_E$). Otherwise, we must treat nearby eigenvalues as degenerate, thus limiting the precision to which we can estimate β by the uncertainty σ_E . We note that to resolve a *particular* E_n to precision σ_E , the number of measurements required scales as $\mathcal{N} \sim 1/(\sigma_E^2 P_n)$, where $1/\sigma_E \gtrsim 1/s$. Thus, the total number of measurements to estimate β to precision σ_E is bound by $\sum_{i=0}^1 \mathcal{N}_i$, where $\mathcal{N}_i \sim \min(1/(\sigma_E^2 P_{n_i}))$ for $i = 0, 1$ and the minimisation is over all known values of degeneracies g_n .

With a known g_{n_0} and temperature, the full set of degeneracies $\{g_n\}$ can be found using $g_n = P_n g_{n_0} \exp(\beta(E_n - E_{n_0}))/P_{n_0}$. Measuring this for a range of β enables reconstruction of the full partition function using $Z(\beta) = \sum_n g_n \exp(-\beta E_n)$. With access to the partition function and temperature, important thermodynamical quantities such as free energies, heat capacities [39] and von Neumann entropy can also be reconstructed.

An important application is in understanding the free energy landscape of a physical system. The Jarzynski equality [40] and its quantum counterpart [41, 42] connect the free energy difference between two thermal states of a system to the work done W in a far-from-equilibrium process. Since it is possible to sample the probability distribution of work done on a quantum system $P(W)$, it has been proposed that the free energy difference can be extracted from $P(W)$. However, this method for extracting free energy differences is not always efficient, for instance, when large negative values of work are involved and at low temperatures [43]. However, by probing $\{E_n\}$ and $\{P_n\}$ directly using our model, we see that $F(\beta) = -\log(Z(\beta))/\beta$ can still be recovered efficiently in those regimes. It is also possible to reconstruct the heat capacity $C = \beta^2 \partial^2 \log(Z(\beta))/\partial \beta^2$ using this method, which can be used to probe quantum critical points [44].

It is also possible to probe thermodynamical quantities of systems that are perturbed far from equilibrium. In particular, we can study the average work performed on a system due to a sudden quench in the interaction Hamiltonian. Further, we can determine the irreversible portion of this work $\langle W_{\text{irr}} \rangle$ [41, 45, 46], which is defined as the difference between $\langle W \rangle$, average work done on the system during the quench, and ΔF , the change in the free energy had the system evolved adiabatically from the thermal state of the initial interaction Hamiltonian to that of the final interaction Hamiltonian. The irreversible work, motivated by the fluctuation theorems and its connections with various entropy measures [41, 47], is a widely-used measure of irreversibility, and has been shown to be a signature for some second-order phase transitions [48]. Note that the average work is also an interesting quantity to study in its own right, and its behaviour across a critical point has been connected to first-order quantum phase transitions [48].

Consider initial and final interaction Hamiltonians $H_{\text{int}}^{(0)}$ and $H_{\text{int}}^{(1)}$, satisfying $H_{\text{int}}^{(0)}, H_{\text{int}}^{(1)} \gg H_0/g$. The change in free energy ΔF may be calculated as above by using the qumode to probe the free energies of the respective thermal states ρ_{Θ_0} and ρ_{Θ_1} of the interaction Hamiltonians. Under a quench, the system state is unchanged, and remains in the initial thermal state ρ_{Θ_0} . Thus, the average work done by the quench is given by $\langle W \rangle = \text{Tr}(\rho_{\Theta_0} H_{\text{int}}^{(1)}) - \text{Tr}(\rho_{\Theta_0} H_{\text{int}}^{(0)}) = \sum_m E_m^{(1)} P_m^{(1)} - \sum_n E_n^{(0)} P_n^{(0)}$, where $E^{(i)}$ and $P^{(i)}$ are energies and probability amplitudes of the state ρ_{Θ_0} under $H_{\text{int}}^{(i)}$ for $i = 0, 1$. These quantities can be determined by the qumode probe, and hence one can calculate the average work along with its irreversible portion.

Finally, we remark that it is also possible to use the qumode probe to find the overlaps of the ground states of a parameter-dependent Hamiltonian at two different values of the parameter λ . This quantity has been used to characterise regions of criticality defining quantum phase transitions in the Dicke model [49]. For pure states, the overlap probability is just the state fidelity between

the ground states. Let $H_{\text{int}}(\lambda = \lambda_c)$ be the interaction Hamiltonian at the quantum critical point. Then the state fidelity of ground states of $H_{\text{int}}(\lambda < \lambda_c)$ and $H_{\text{int}}(\lambda > \lambda_c)$ can be measured by concatenating two qumode probe quantum circuits. The first qumode probe circuit evolves under $H_{\text{int}}(\lambda < \lambda_c)$ and is used to prepare the ground state $|u_{\lambda < \lambda_c}\rangle$ of $H_{\text{int}}(\lambda < \lambda_c)$. Now we use $|u_{\lambda < \lambda_c}\rangle$ as the state input to the second qumode probe circuit, which now evolves under $H_{\text{int}}(\lambda > \lambda_c)$. The final probability of obtaining a zero eigenvalue is then $P_0 = |\langle u_{\lambda < \lambda_c} | u_{\lambda > \lambda_c} \rangle|^2$, which is the sought after overlap probability.

Candidates for Experimental Implementations.

We now suggest some current experimental setups that would be ideal candidates to test our protocol. We consider two interaction Hamiltonians, the quantum Rabi model and the Dicke model, both of which describe light-matter interactions, and are hence ubiquitous in quantum technologies.

The first Hamiltonian, the quantum Rabi model, is given by [36]

$$H_{QR} = gx \otimes \sigma_x, \quad (9)$$

where σ_x is the usual Pauli x matrix [6], taking the role of the interaction Hamiltonian H_{int} . The Hamiltonian was originally conceived as a description of a quantised light field interacting with a two-level system. One often finds this Hamiltonian in its simplified guise as the Jaynes-Cummings Hamiltonian, where the approximation is made to neglect the counter-rotating terms $a\sigma^-$ and $a^\dagger\sigma^+$; nevertheless, systems described by this Hamiltonian are typically more accurately described by the full Rabi Hamiltonian.

As noted above, the majority of current quantum technologies involve light-matter interactions, and so one can find many examples of systems utilising such interactions. Sometimes, as with ion traps [2], Rydberg atoms [50], and laser-driven tunnelling of ultracold atoms in optical lattice [51], the continuous variable mode is treated as a classical field (although in the case of the former, interactions between the internal states of the ions and their quantised motional state is well-described by the above Hamiltonian). In principle, our protocol can be applied to such systems by replacement of the classical light with a qumode light field, though to achieve similar transition rates one would need either a highly-populated field, or a very strong coupling. While being optimistic about such possibilities, we shall for concreteness highlight examples where the fully-quantum interaction is realised.

Both cavity [52, 53] and circuit [54–56] quantum electrodynamics experiments consist of interactions between a continuous variable mode (cavity fields in the former, nanomechanical resonators in the latter) and a two-level system (atoms and superconducting qubits respectively), interacting through a quantum Rabi Hamiltonian Eq. (9) in the (ultra)strong coupling regime. Such setups operate in a regime where the qumode measurement resolution can be much finer than the differences between the inter-

action Hamiltonian eigenvalues, which for this example is of order unity. For example, in Ref. [55] the coupling between qubit and resonator gives $g \approx 10^{10}$, and the Q-factor of 10^3 and resonance frequency of 8.2GHz leads to $g\tau \sim 200$ when the protocol is run for times of the order of the resonator lifetime. With the parameters of Ref. [53], we would have $g\tau = 40$ when τ is the cavity lifetime. Thus, for both these examples, the spread σ_E would be much smaller than the differences between the measured eigenvalues.

While Eq. (9) makes it clear that the protocol can be used to probe moments of σ_x for a two-level system, it can straightforwardly be applied more generally. First, the physical motivation and derivation of the Hamiltonian does not necessarily require that the system has only two states, and can be rederived for any number of states, by replacing σ_x with the appropriate x spin operator for the number of states. Secondly, by illuminating an array of such systems with the same light field, the Hamiltonian becomes an interaction between the light field and the sum of the individual spin operators for each system, and thus probes moments of the total spin operator, as well as correlations between individual spins. Finally, it is possible to probe the spin operator in any chosen direction, by appropriate rotation of the individual spins prior to probing (e.g. applying a Hadamard gate [6] to the system allows probing of σ_z).

A related Hamiltonian that takes the desired form is the Dicke model, which describes the interaction between an ensemble of identical two-level atoms interacting with a common quantised light field. It is given by

$$H_D = gx \otimes J_x, \quad (10)$$

where \mathbf{J} is a spin operator describing the collective excitations of the ensemble. The model has been realised experimentally with cold atoms trapped in an optical cavity, in the context of studying quantum phase transitions [57]. Here, we see it also as a possible route to non-destructively probe atomic ensembles. This setting is particularly apt for our proposal, as the inclusion of the optical cavity facilitates the use of tools from quantum optics, which constitutes a primary manifestation of continuous variable quantum systems. The strong light-matter coupling and long cavity lifetimes achievable in such systems provide favourable conditions for testing our protocol. Specifically, a ratio of 0.2 for the collective interaction strength to cavity decay rate has been achieved [57], corresponding to $g\tau \sim \mathcal{O}(10^{-3} - 10^{-2})$ when the protocol is run for a time comparable to the cavity lifetime. This allows for measurement of the number of atomic excitations to be resolved to within a few hundred even with no squeezing. This is quite sharp when compared to the total number of atoms (10^5). Further, we note extensions of the above experiment have succeeded in additional manipulation of the trapped atoms, by confining them to various lattice structures [58].

Discussion. We have shown that properties of quantum systems may be imprinted onto continuous variable

qumode ancillae to allow for non-destructive probing of the system. For an appropriate choice of interaction operator and initial qumode state, the spectrum of the desired observable, and the occupation probabilities of its eigenstates for a particular system state are mapped directly on to the qumode state. The qumode state then behaves according to the same statistics as this operator, and thus measurement of the qumode reproduces the same result as a direct measurement of the system would, while avoiding particular drawbacks associated with direct measurements of practical implementations of quantum technologies. Further, the direct recovery of the measurement statistics is in contrast to analogous protocols with qubit ancillae, where one must first employ post-processing such as taking derivatives [26] or Fourier transforms [19, 20, 27] of the measurement outcomes. As our proposal is feasible with typical parameters for contemporary experiments, it could find immediate use in the field.

We note that while qumode probes are non-destructive to the system, in general they will not be non-demolition. The backaction on the system state will project it to the eigenstate (or in the case of degeneracies, eigenspace) associated with the measurement outcome, in much the same way as a direct measurement of the system would. For an interaction operator with the eigenstates known, this projection could perhaps be employed as a form of probabilistic state engineering [59–62], with the particular state created being heralded by the qumode measurement outcome, potentially adding further utility to the addition of our protocol to the quantum technologies toolbox.

After completion of this manuscript, we became aware of a recent work employing a qumode-based protocol to measure thermodynamical work [63].

Acknowledgements. The authors acknowledge financial support from Singapore National Research Foundation Awards NRF-NRFF2016-02 and NRF-NRFF2013-01, the Engineering and Physical Sciences Research Council (Doctoral Training Account), John Templeton Foundation Grant 53914 “Occam’s quantum mechanical razor: Can quantum theory admit the simplest understanding of reality?”, and the Clarendon Fund, Merton College of the University of Oxford. T.J.E. thanks the Centre for Quantum Technologies, National University of Singapore for their hospitality.

Technical Appendix

Here we derive Eq. (3) which gives the probability of the momentum measurement resulting in the outcome $|p\rangle$, denoted $P(p)$, when the initial state is infinitely squeezed. Recall that for a qumode prepared in a given state $G(x)$, its state after interacting with the system for a time τ is given by Eq. (2), which we reproduce here for

convenience:

$$\rho_q(t) = \int \int dx dx' G(x) G^*(x') L(x, x', \tau) |x\rangle \langle x'|, \quad (11)$$

with $L(x, x', \tau) = \sum_n P_n \exp(-ig(x - x') E_n \tau)$.

For the infinitely squeezed initial state we then have

$$\begin{aligned} P(p) &= \langle p | \rho_q(\tau) | p \rangle \\ &= \frac{1}{(2\pi)^2} \int \int dx dx' e^{i(x-x')(p_0-p)} L(x, x', \tau) \\ &= \frac{1}{(2\pi)^2} \sum_n P_n \int \int dx dx' e^{i(x-x')(p_0-p-gE_n\tau)} \\ &= \sum_n P_n (\delta(p - (p_0 - gE_n\tau)))^2, \end{aligned} \quad (12)$$

as given in Eq. (3).

We also derive Eqs. (5) and (7), which describe the sampled probability distribution when the initial state has a finite bin size, or is finitely squeezed. Inserting the explicit initial qumode state for a finite bin of size L , $G(x) = 1/(\sqrt{2\pi L}) \int_{-\frac{L}{2}}^{\frac{L}{2}} dk \exp(i(p_0 + k)x)$, we have that

$$\begin{aligned} \rho_q(\tau) &= \frac{1}{2\pi L} \sum_n P_n \int \int dx dx' \int_{-\frac{L}{2}}^{\frac{L}{2}} \int_{-\frac{L}{2}}^{\frac{L}{2}} dk dk' \\ &\quad \times e^{i(p_0+k)x - i(p_0+k')x' - ig(x-x')E_n\tau} |x\rangle \langle x'|. \end{aligned} \quad (13)$$

Thus, we have that

$$\begin{aligned} P(p) &= \frac{1}{(2\pi)^2 L} \sum_n P_n \int \int dx dx' \int_{-\frac{L}{2}}^{\frac{L}{2}} \int_{-\frac{L}{2}}^{\frac{L}{2}} dk dk' \\ &\quad \times e^{i(p_0-p+k)x - i(p_0-p+k')x' - ig(x-x')E_n\tau} \\ &= \frac{1}{(2\pi)^2 L} \sum_n P_n \int dx \int_{-\frac{L}{2}}^{\frac{L}{2}} dk e^{i(p_0-p+k-gE_n\tau)x} \\ &\quad \times \int dx' \int_{-\frac{L}{2}}^{\frac{L}{2}} dk' e^{-i(p_0-p+k'-gE_n\tau)x'} \\ &= \frac{1}{L} \sum_n P_n \left(\int_{-\frac{L}{2}}^{\frac{L}{2}} dk \delta(p - (p_0 - gE_n\tau + k)) \right)^2 \\ &= \sum_n \begin{cases} \frac{P_n}{L} & -\frac{L}{2} \leq p - p_0 + gE_n\tau \leq \frac{L}{2} \\ 0 & \text{otherwise,} \end{cases} \end{aligned} \quad (14)$$

in agreement with Eq. (5).

We now do the same for the finite squeezed state, which has initial wavefunction $G(x) = (s^2/\pi)^{\frac{1}{4}} (1/\sqrt{2\pi}) \exp(ip_0 x) \int dq \exp(-s^2 q^2/2)$. The state of the qumode after the interaction for time τ is given by

$$\begin{aligned} \rho_q(t) &= \frac{s}{\sqrt{\pi}} \frac{1}{2\pi} \sum_n P_n \int \int dx dx' \int \int dq dq' \\ &\quad \times e^{i(p_0+q)x - i(p_0+q')x' - ig(x-x')E_n\tau} e^{-\frac{s^2(q^2+q'^2)}{2}} |x\rangle \langle x'|, \end{aligned} \quad (15)$$

and the associated probability distribution is given by

$$\begin{aligned}
 P(p) &= \frac{s}{4\pi^{\frac{5}{2}}} \sum_n P_n \int dx \int dq e^{i(p_0 - p + q - gE_n\tau)x} e^{-\frac{s^2 q^2}{2}} \\
 &\quad \times \int dx' \int dq' e^{-i(p_0 - p + q' - gE_n\tau)x'} e^{-\frac{s^2 q'^2}{2}} \\
 &= \frac{s}{\sqrt{\pi}} \sum_n P_n \left(\int dq \delta(p - (p_0 - gE_n\tau + q)) e^{-\frac{s^2 q^2}{2}} \right)^2 \\
 &= \frac{s}{\sqrt{\pi}} \sum_n P_n e^{-s^2(p - p_0 + g\tau E_n)^2}, \tag{16}
 \end{aligned}$$

as given in Eq. (7). In the limit of infinite squeezing, this reduces to Eq. (3).

-
- [1] I. Bloch, J. Dalibard, and S. Nascimbène, *Nat. Phys.* **8**, 267 (2012).
- [2] R. Blatt and C. F. Roos, *Nat. Phys.* **8**, 277 (2012).
- [3] J. Clarke and F. K. Wilhelm, *Nature* **453**, 1031 (2008).
- [4] J. M. Raimond, M. Brune, and S. Haroche, *Rev. Mod. Phys.* **73**, 565 (2001).
- [5] C. Monroe, *Nature* **416**, 238 (2002).
- [6] M. A. Nielsen and I. L. Chuang, *Quantum Computation and Quantum Information* (Cambridge University Press, 2010).
- [7] V. Giovannetti, S. Lloyd, and L. Maccone, *Nat. Photon.* **5**, 222 (2011).
- [8] M. Lewenstein, A. Sanpera, and V. Ahufinger, *Ultracold Atoms in Optical Lattices: Simulating Quantum Many-Body Systems* (Oxford University Press, Oxford, England, 2012).
- [9] S. Haroche and J. M. Raimond, *Exploring the Quantum: Atoms, Cavities, and Photons* (OUP Oxford, 2013).
- [10] Z. Hadzibabic, S. Gupta, C. A. Stan, C. H. Schunck, M. W. Zwierlein, K. Dieckmann, and W. Ketterle, *Phys. Rev. Lett.* **91**, 160401 (2003).
- [11] E. Altman, E. Demler, and M. D. Lukin, *Phys. Rev. A* **70**, 013603 (2004).
- [12] S. Fölling, F. Gerbier, A. Widera, O. Mandel, T. Gericke, and I. Bloch, *Nature* **434**, 481 (2005).
- [13] I. Bloch, J. Dalibard, and W. Zwerger, *Rev. Mod. Phys.* **80**, 885 (2008).
- [14] A. Recati, P. O. Fedichev, W. Zwerger, J. Von Delft, and P. Zoller, *Phys. Rev. Lett.* **94**, 40404 (2005).
- [15] M. Bruderer and D. Jaksch, *New J. Phys.* **8**, 87 (2006).
- [16] J. Goold, T. Fogarty, N. L. Gullo, M. Paternostro, and T. Busch, *Phys. Rev. A* **84**, 063632 (2011).
- [17] M. Knap, A. Shashi, Y. Nishida, A. Imambekov, D. A. Abanin, and E. Demler, *Phys. Rev. X* **2**, 041020 (2012).
- [18] P. Haikka, S. McEndoo, and S. Maniscalco, *Phys. Rev. A* **87**, 012127 (2013).
- [19] L. Mazzola, G. De Chiara, and M. Paternostro, *Phys. Rev. Lett.* **110**, 230602 (2013).
- [20] R. Dorner, S. R. Clark, L. Heaney, R. Fazio, J. Goold, and V. Vedral, *Phys. Rev. Lett.* **110**, 230601 (2013).
- [21] C. Sabín, A. White, L. Hackermuller, and I. Fuentes, *Sci. Rep.* **4**, 6436 (2014).
- [22] L. Fusco, S. Pigeon, T. J. G. Apollaro, A. Xuereb, L. Mazzola, M. Campisi, A. Ferraro, M. Paternostro, and G. De Chiara, *Phys. Rev. X* **4**, 031029 (2014).
- [23] T. B. Batalhão, A. M. Souza, L. Mazzola, R. Auccaise, R. S. Sarthour, I. S. Oliveira, J. Goold, G. De Chiara, M. Paternostro, and R. M. Serra, *Phys. Rev. Lett.* **113**, 140601 (2014).
- [24] D. Hangleiter, M. T. Mitchison, T. H. Johnson, M. Bruderer, M. B. Plenio, and D. Jaksch, *Phys. Rev. A* **91**, 013611 (2015).
- [25] F. Cosco, M. Borrelli, F. Plastina, and S. Maniscalco, *Phys. Rev. A* **95**, 053620 (2017).
- [26] T. J. Elliott and T. H. Johnson, *Phys. Rev. A* **93**, 043612 (2016).
- [27] T. H. Johnson, F. Cosco, M. T. Mitchison, D. Jaksch, and S. R. Clark, *Phys. Rev. A* **93**, 053619 (2016).
- [28] A. Bermudez, G. Aarts, and M. Müller, arXiv preprint arXiv:1704.02877 (2017).
- [29] E. Bentine, T. L. Harte, K. Luksch, A. J. Barker, J. Mur-Petit, B. Yuen, and C. J. Foot, *J. Phys. B* **50**, 094002 (2017).
- [30] S. Lloyd and S. L. Braunstein, *Phys. Rev. Lett.* **82**, 1784 (1999).
- [31] S. L. Braunstein and P. Van Loock, *Rev. Mod. Phys.* **77**, 513 (2005).
- [32] A. Furusawa and P. Van Loock, *Quantum teleportation and entanglement: a hybrid approach to optical quantum information processing* (John Wiley & Sons, 2011).
- [33] C. Weedbrook, S. Pirandola, R. García-Patrón, N. J. Cerf, T. C. Ralph, J. H. Shapiro, and S. Lloyd, *Rev. Mod. Phys.* **84**, 621 (2012).
- [34] U. L. Andersen, J. S. Neergaard-Nielsen, P. van Loock, and A. Furusawa, *Nat. Phys.* **11**, 713 (2015).
- [35] N. Liu, J. Thompson, C. Weedbrook, S. Lloyd, V. Vedral, M. Gu, and K. Modi, *Phys. Rev. A* **93**, 052304 (2016).
- [36] C. Gerry and P. Knight, *Introductory Quantum Optics* (Cambridge University Press, 2005).
- [37] L. A. Correa, M. Mehboudi, G. Adesso, and A. Sanpera, *Phys. Rev. Lett.* **114**, 220405 (2015).
- [38] T. M. Stace, *Phys. Rev. A* **82**, 011611 (2010).
- [39] M. Glazer and J. Wark, *Statistical Mechanics* (Oxford University Press, 2002).
- [40] C. Jarzynski, *Phys. Rev. Lett.* **78**, 2690 (1997).
- [41] H. Tasaki, arXiv preprint arXiv:cond-mat/0009244 (2000).
- [42] S. Mukamel, *Phys. Rev. Lett.* **90**, 170604 (2003).
- [43] A. J. Roncaglia, F. Cerisola, and J. P. Paz, *Phys. Rev. Lett.* **113**, 250601 (2014).
- [44] T. Liang, S. M. Koohpayeh, J. W. Krizan, T. M. McQueen, R. J. Cava, and N. P. Ong, *Nat. Comm.* **6** (2015).
- [45] M. Campisi, P. Hänggi, and P. Talkner, *Rev. Mod. Phys.* **83**, 771 (2011).

- [46] R. Dorner, J. Goold, C. Cormick, M. Paternostro, and V. Vedral, Phys. Rev. Lett. **109**, 160601 (2012).
- [47] S. Deffner and E. Lutz, Phys. Rev. Lett. **105**, 170402 (2010).
- [48] E. Mascarenhas, H. Bragan  , R. Dorner, M. F. Santos, V. Vedral, K. Modi, and J. Goold, Phys. Rev. E **89**, 062103 (2014).
- [49] P. Zanardi and N. Paunkovi  , Phys. Rev. E **74**, 031123 (2006).
- [50] E. Urban, T. A. Johnson, T. Henage, L. Isenhower, D. D. Yavuz, T. G. Walker, and M. Saffman, Nat. Phys. **5**, 110 (2009).
- [51] D. Jaksch and P. Zoller, New J. Phys. **5**, 56 (2003).
- [52] S. Gleyzes, S. Kuhr, C. Guerlin, J. Bernu, S. Deleglise, U. B. Hoff, M. Brune, J.-M. Raimond, and S. Haroche, Nature **446**, 297 (2007).
- [53] C. Hamsen, K. N. Tolazzi, T. Wilk, and G. Rempe, Phys. Rev. Lett. **118**, 133604 (2017).
- [54] M. D. LaHaye, J. Suh, P. M. Echternach, K. C. Schwab, and M. L. Roukes, Nature **459**, 960 (2009).
- [55] P. Forn-D  az, J. Lisenfeld, D. Marcos, J. J. Garc  a-Ripoll, E. Solano, C. J. P. M. Harmans, and J. E. Mooij, Phys. Rev. Lett. **105**, 237001 (2010).
- [56] F. Yoshihara, T. Fuse, S. Ashhab, K. Kakuyanagi, S. Saito, and K. Semb  , Nat. Phys. **13**, 44 (2017).
- [57] K. Baumann, C. Guerlin, F. Brennecke, and T. Esslinger, Nature **464**, 1301 (2010).
- [58] R. Landig, L. Hruba, N. Dogra, M. Landini, R. Mottl, T. Donner, and T. Esslinger, Nature (2016).
- [59] F. Verstraete, M. M. Wolf, and J. I. Cirac, Nat. Phys. **5**, 633 (2009).
- [60] M. K. Pedersen, J. J. W. H. S  rensen, M. C. Tichy, and J. F. Sherson, New J. Phys. **16**, 113038 (2014).
- [61] T. J. Elliott, W. Kozlowski, S. F. Caballero-Benitez, and I. B. Mekhov, Phys. Rev. Lett. **114**, 113604 (2015).
- [62] C. Joshi, J. Larson, and T. P. Spiller, Phys. Rev. A **93**, 043818 (2016).
- [63] F. Cerisola, Y. Margalit, S. Machluf, A. J. Roncaglia, J. P. Paz, and R. Folman, arXiv preprint arXiv:1706.07866 (2017).